Proceedings of OMAE'02
21st International Conference on Offshore Mechanics and Arctic Engineering
June 23-28, 2002,Oslo, Norway

OMAE2002-28073

DYNAMIC RESPONSE OF SHALLOW WATER MONOPOD PLATFORMS

Micaela Pilotto
Centre for Oil and Gas Engineering
The University of Western Australia
Crawley, Western Australia, 6009
Australia

Beverley F. Ronalds
Centre for Oil and Gas Engineering
The University of Western Australia
Crawley, Western Australia, 6009
Australia

Roman Stocker
Centre for Water Research
The University of Western Australia
Crawley, Western Australia, 6009
Australia

ABSTRACT

This paper describes a systematic desktop study of the non-linear dynamic behavior of monopod platforms. The aim of this work is to highlight some important factors in the dynamics of minimum structures in shallow water. The analysis is performed in the time domain with regular wave loading. The non-linearities are due to the wave theory (Stream function of 8th order), to the shallow water environment and to the drag-dominated situation. Idealizations of two braced monopod configurations are compared with the simpler and more commonly studied unbraced monopod. Aspects highlighted for each configuration include the effect of wave period and top mass on the dynamic amplification factor. In particular, the analysis focuses on the highly non-linear behavior in the wave zone.

The results show that braced monopods are dynamically more sensitive than unbraced monopods. In particular, braced monopods exhibit more energy at higher harmonics in the quasi-static response. This yields a consistently stronger dynamic response even if the wave period and the natural period of the structure are very different. The importance of the mass at the top of the structure in the dynamic response and in particular its role in increasing the dynamic amplification factor up the water column are highlighted.

Key words: non-linear dynamics, monopod, dynamic amplification factor, Stream function

INTRODUCTION

Minimum structures such as mono-towers and braced monopods are widely used in Australia's North West Shelf. The dynamic behavior of these structures with a braced lower structure is complicated by several factors. First, such structures are generally located in relatively shallow water, where non-linear wave kinematics are important, especially in harsh environments. Second, unlike most fixed platforms, their configuration is such that the fundamental dynamic bending behavior is concentrated in the wave zone, rather than throughout the water column.

The importance of this highly non-linear wave zone has been illustrated by Ronalds *et al*. (2000). Previous studies have focused on the relationship between the maximum quasi-static environmental load and the maximum wave height, expressed by the wave height exponent α (Tuty *et al*., 2001b). Research has confirmed that α varies with platform water depth, structural configuration and member diameters (Ronalds *et al*., 2001; Tuty *et al*., 2001a), showing that drag-dominated platforms are more likely to experience larger values of α (reaching the value of four, or more, in comparison with the usual value of two for drag-dominated structures) higher up the

water column. This demonstrates that the wave zone is a sensitive region. Indeed, the failure of a braced monopod (Campbell) on the North West Shelf during a tropical cyclone was localized in the wave zone (Ronalds *et al*.,1998).

The previous studies are based on quasi-static results. On the other hand the dynamic approach yielded interesting insight into the behavior of braced monopods in the North Sea (Nedergaard *et al.,* 1996) and of jack-ups units (Williams *et al.,* 1999).

The dynamic approach is pursued in this paper, with a particular focus on minimum structures in a North West Shelf environment. By analyzing the energy content at different harmonics and the dynamic amplification factor of lateral displacements and bending moments, we show that these structures exhibit an inherently different dynamic behavior compared to the single degree of freedom case and therefore require a comprehensive dynamic analysis.

WAVE THEORIES AND FORCES

We consider here a typical monopod location on Australia's North West Shelf. The water depth is 42.3 m and no currents or wind are acting. Generally, monopods are slender structures which, together with the shallow water environment, causes drag forces (F_d) to dominate over inertia forces (F_i). For a given wave height and water depth, the ratio F_d / F_i depends on the diameter of the caisson. This is typically between 1.2 to 5 m, depending on where the conductors and risers are positioned (Tuty *et al*., 2001a). As a representative value for monopods we investigate a structure of 1.8 m diameter. Figure 1 shows how these structures can be considered to be drag dominated, having maximum F_d / F_i values between 1.5 and 6.

The non-linearity of the drag term $u \cdot |u|$, where u is the horizontal wave velocity in Morison's formula, has the effect of introducing changes in the statistics and in the frequency content of the forcing. Statistical changes have been studied for example by Pierson and Holmes (1965) and Borgman (1969) and are not addressed in this paper. For the purpose of determining the dynamic behavior, the frequency content of the forcing will be outlined briefly. It is known that the $u \cdot |u|$ term introduces two important harmonics in the forcing F_d, one at the wave frequency f_w and one at $3f_w$ (Baltrop and Adams, 1991).

Hereafter we investigate another mechanism which is shown to be responsible for the introduction of new harmonics in F_d, namely the non-linear motion of the free surface. We consider the simple case of a vertical cylinder of 1 m diameter in 42.3 m of water. From Fig. 1 it can be seen that this configuration has $F_d / F_i = 7$, so we can concentrate only on the drag force. For simplicity, wave velocities have been calculated following Airy's linear theory. The characteristics of the wave are those shown in Table 1. These data refer to the Wandoo location, on the North West Shelf.

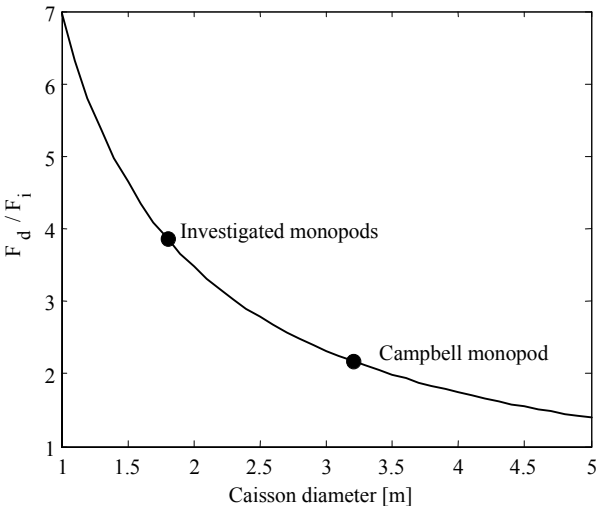

Figure 1 Ratio of drag and inertia forces for different caisson diameters using environmental parameters from Table 1.

Water depth [m]	Wave period [s]	Wave height [m]
42.3	12.5	20.9

Table 1 Wave characteristics of the Wandoo location (North West Shelf) for a 100 year return period

The integral $\hat{F}_d$ of Morison's drag force F_d over the depth of the water column is defined as:

$$\hat{F}_d \propto \int_0^{h+\eta(t)} u(t) \cdot |u(t)| \cdot dz \qquad (1)$$

where h is the water depth and $\eta(t)$ is the water elevation. Since we are only interested in the frequency content of $\hat{F}_d$, the proportionality factors in (1) have been neglected. The power spectral density (PSD) of $\hat{F}_d$ has been computed using Welch's algorithm. Four energy peaks (at f_w, $2f_w$, $3f_w$ and $4f_w$) are observed instead of the two expected from the non-linearity in $u \cdot |u|$ (at f_w and $3f_w$). In Fig. 2 these peaks are nondimensionalized by the energy of the first peak (the one at f_w) and are represented as functions of H/h, where H is the wave height. It can be seen how the second and fourth peaks become more important in shallow water, where the wave approaches the water depth until limited by wave breaking.

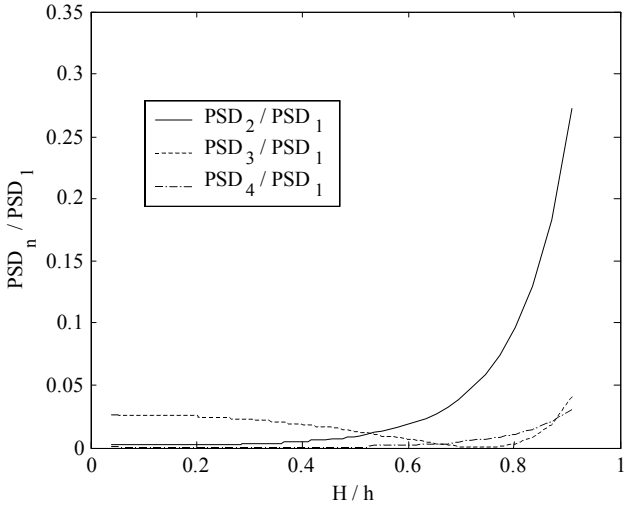

Figure 2 Energy of the 2nd, 3rd and 4th peaks of the power spectral density of the drag force (PSD_n), normalized by the maximum value of the energy of the 1st peak (PSD_1)

Therefore a drag-dominated structure in shallow water, forced by a linear monochromatic wave, is in fact subject to a force having four important harmonics. This means that even if the period of the wave and the natural period of the structure are very different, the structure could be dynamically sensitive to the wave load if the two periods are in a ratio of 2:1, 3:1 or 4:1, in which case one of the higher harmonics can excite the dynamic behavior of the structure. If the structure is inertia dominated and in deep water, on the other hand, these non-linearities do not arise, since the inertia term in Morison's formula is linearly dependent on the wave height.
Similar arguments apply for any other deterministic wave. In our case the Stream Function of 8th order has been used and each of the eight fundamental harmonics develops frequency changes in shallow water, as illustrated for the linear wave. Determining the exact frequency contents is beyond the scope of this paper.

METHOD OF ANALYSIS

Description of the models

Three different models are considered to compare a range of minimum structures (Fig. 3). The models have been kept simple on purpose to highlight some trends in monopod behavior. Model 1 is the most commonly analyzed single vertical cylinder, restrained at the mud-line. It should be noted that Model 1 is too flexible to be considered a realistic model for a monopod in this water depth, and it is included in the analysis mainly for the purpose of comparison with the other more realistic models. Model 2 is also a vertical cylinder, restrained at the height of the apex, the point where the braced substructure starts. This is to simulate a case with substantial stiff bracing below the apex. Model 3 is a simple 3D braced monopod with the apex in the same position as Model 2. Apex location (31 m) and water depth (42.3 m) have been chosen following examples on the North West Shelf.

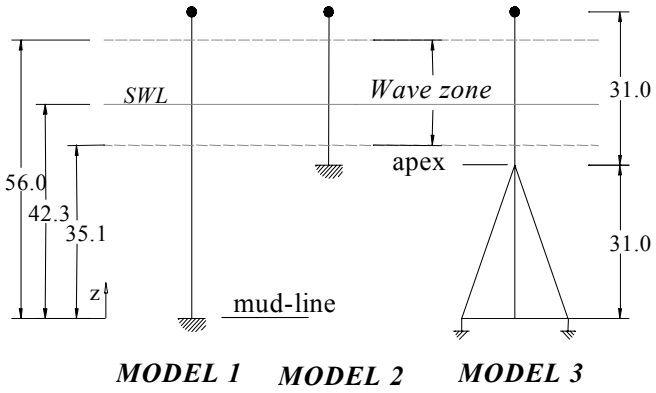

Figure 3 Geometric characteristics of the three models and of the wave considered

All models have the same caisson section with a diameter of 1.8 m and the same material characteristics and damping ratio (ξ=1.5%). We have chosen to impose the fundamental natural period (T_n = 2.5 s) to be the same for all the models by varying the lumped mass at the top of the structure (see Table 2) in order to consistently compare their dynamic behavior. A study of the influence of the mass at the top of the structure on its dynamic behavior has also been carried out by changing the mass at the top of Model 1 and is presented in a later section. The natural period has been chosen so that $T_w / T_n = f_n / f_w = 5$, which is not untypical for minimum structures, where T_w and f_w are, respectively, the wave period and frequency, while T_n and f_n are the natural period and frequency of the structure. For wave characteristics see Table 1.

	Top mass [t]	Structure mass [t]
Model 1	6.6	86.5
Model 2	220.9	43.2
Model 3	118.6	189.7

Table 2 Masses of the models

A sensitivity study has been conducted to show how the number of nodes used for discretizing the structure influences the dynamic behavior. This sensitivity study has been carried out for the dynamic amplification factor (*DAF*), since this will be taken as an indicator of the importance of the dynamics in the remainder of the paper. The *DAF* is defined as the ratio of the maximum dynamic response versus the maximum static response. Figure 4 shows how the *DAF* of the displacements at

the top of Model 1 varies as a function of the number of nodes down the caisson. The increase in the *DAF* with the number of nodes can be explained by considering that a large number of nodes gives the structure a large number of degrees of freedom which, in turn, allows a more accurate dynamic response. The dynamic response appears to be fully developed when ten or more nodes are considered. The reason is that ten elements are needed in order to model the shape function for the first natural mode of the structure. These considerations are particularly relevant if one considers that it is often common design practice to use the single degree of freedom model (a single mass at the top and a weightless caisson). We chose to use the minimum number of elements (ten) necessary to achieve a stable estimate of the *DAF*.

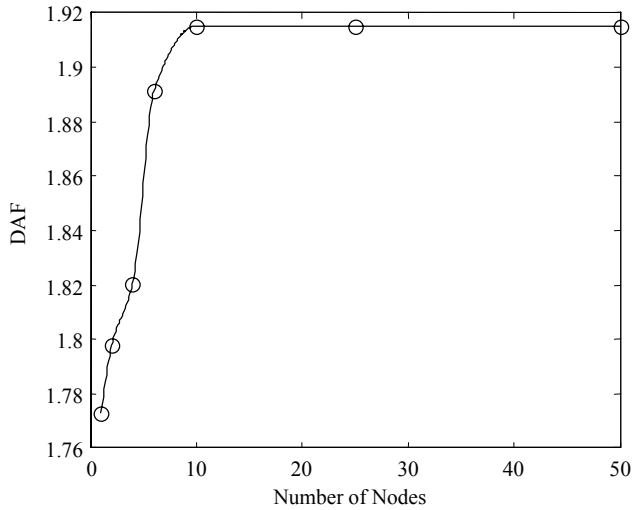

Figure 4 *DAF* of displacements versus the number of nodes for Model 1

Analysis

The analysis has been performed quasi-statically and dynamically using SESAM with wave kinematics predicted by the Stream function theory of 8th order. The quasi-static approach will be referred to as "static" hereafter, for simplicity. The wave for 100 years return period has its crest at 56.0 m from the mud-line and the trough at 35.1 m. The top of the structure, then, is always above the maximum wave elevation and the apex is always under the minimum.

The dynamic analysis has been carried out by direct time integration with an integration time step of 0.05 s.

RESULTS

Time series

This section presents results for static and dynamic analyses of the three models in term of caisson displacements and bending moments. Results are presented for the ninth, tenth and eleventh wave cycles to allow transient effects to decay.

Figure 5 shows the lateral deflections at the top of each model for the static and dynamic analysis. Static and dynamic displacements have been nondimensionalized by the maximum static displacement δ_{max}. The dynamic response peaks just after each wave crest has passed. The three models are all dynamically sensitive, since the dynamic displacements are twice or more the static ones. While Model 1 has the largest top deflection, as we could expect from its configuration (Fig. 3), it appears to be less dynamically sensitive than Models 2 and 3.

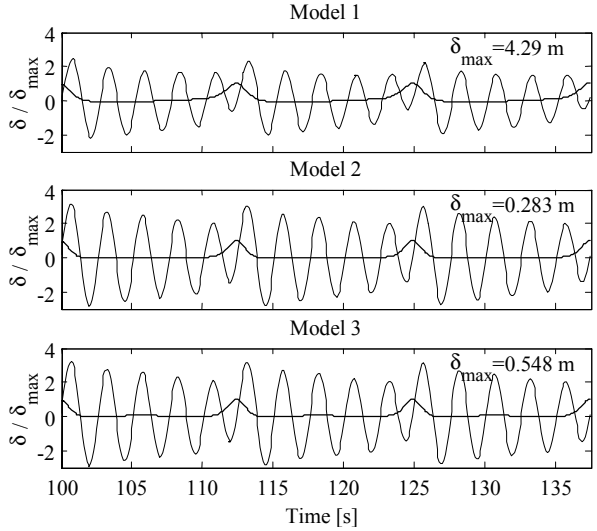

Figure 5 Time series of static and dynamic top displacements δ, normalized by the maximum value of the static displacements, δ_{max}

This can be explained from Fig. 6, where the power spectral density of the static response for the three models is shown. In order to better compare the energies for the three models, the PSD for each model has been divided by the square of its maximum static displacement (δ_{max}). Models 2 and 3 exhibit a more pronounced non-linear behavior than Model 1, since more energy is distributed at high frequencies. Model 3 has a greater energy component in the second harmonic of the wave than the first one. Moreover both Models 2 and 3 have a comparable amount of energy at $f / f_w = 5$. This is important because the energy at that frequency dominates the dynamic response. The different PSD distributions are attributed to the structural configurations of the monopods. As the trough of the wave passes statically through the structure, Model 3 is given a small positive displacement at the deck level (seen in Fig. 5), while Model 1 experiences a negative displacement and Model 2 is little affected due to the fixity at the apex. The double excitation experienced by Model 3 as each wave passes causes the second harmonic to dominate.

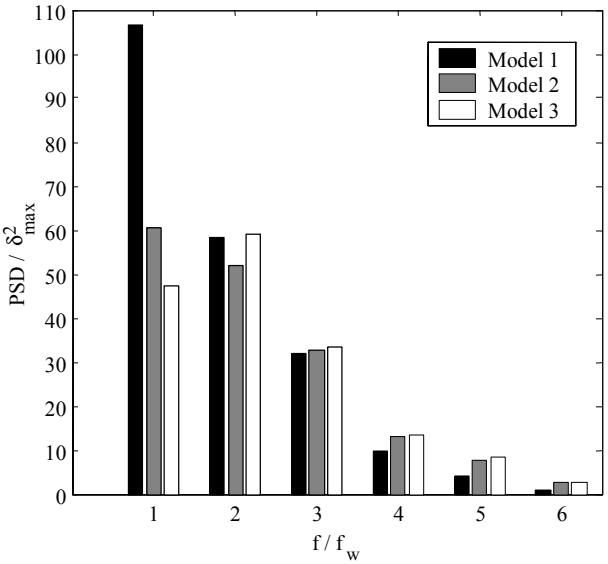

Figure 6 Power spectral density of static displacements divided by the square of the maximum value of the static displacement (δ^2_{max}) for each model

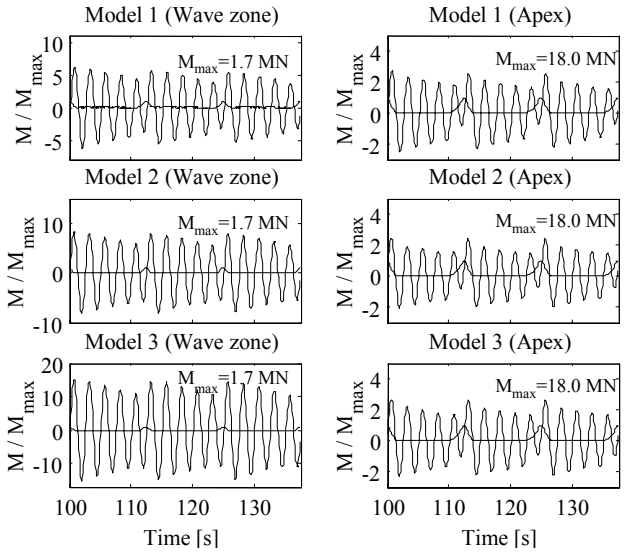

Figure 7 Time series of bending moments *M* at the apex and in the wave zone (*z*=49.6 m), normalized by the maximum static moment M_{max}

Figure 7 presents the static and dynamic moments for each model in the wave zone (49.6m from mud-line) and at the height of the apex, nondimensionalized by the maximum static moment at each location. The static moments are the same for all three models. However, the pattern of static loading is seen to change up the water column due to the effect of partial inundation. This causes the forcing function to become increasingly like a pulse with duration comparable to half the natural period. As for the top displacements of Fig. 5, the response of the structure peaks just after the wave crest has passed. At the apex the dynamic moments are about twice the static ones. The same trend can be noticed as for the displacements of the different models, with Model 3 being more dynamically sensitive than Models 1 and 2. Moreover, up the water column, while the static moments are obviously decreasing, the dynamic moments become five to ten times larger than the static ones. This peculiar behavior of the wave zone, where the dynamic response of the structure is strongly enhanced, is the focus of this paper and is investigated in more detail in the following section in terms of the *DAF*.

Dynamic amplification factor (*DAF*)

To investigate further the behavior highlighted in the previous section we study the dynamic amplification factor, both for displacements and for moments. Figure 8 shows the *DAF* for lateral displacements of the three models as a function of the vertical position in the water column. Two main features are observed. First, the *DAF* increases essentially linearly up the water column. Second, the different slopes of the three lines indicate that the dynamic sensitivity increases considerably faster up the water column for Models 2 and 3, as compared to Model 1. This is due to three reasons. The first is the stronger non-linear behavior of Models 2 and 3, explained in terms of energy distribution in the previous section and illustrated in Fig. 6. The second reason depends on the different magnitude of displacements for the three models. Since Model 1 exhibits larger displacements, and therefore velocities (the natural period being the same) than Models 2 and 3, damping plays a stronger role in the dynamic response of Model 1. The third reason is related to the different masses at the top of each structure, with the *DAF* increasing more rapidly for larger masses.

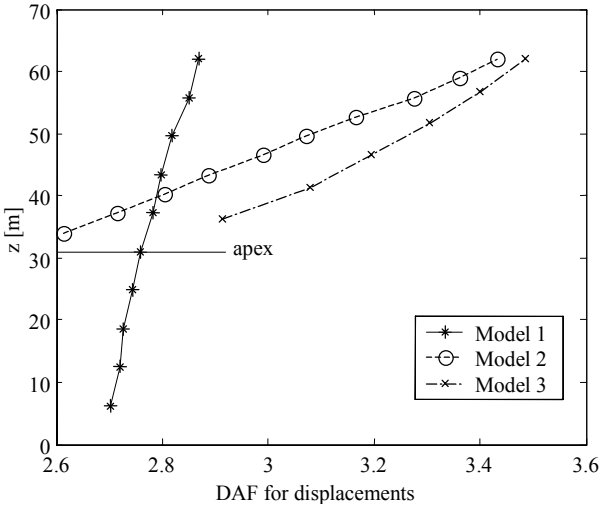

Figure 8 Dynamic amplification factor for displacements as a function of the vertical position in the water column

To better understand how the mass at the top influences the *DAF* of the displacements we suggest the following simplified explanation. In the static analysis the displacements x_s are computed as:

$$Kx_s = F \tag{2}$$

where K is the stiffness and F the forcing function. Dynamic displacements x_d are computed from:

$$M\ddot{x}_d + C\dot{x}_d + Kx_d = F \tag{3}$$

where M is the mass, C the damping and the dot denotes differentiation with respect to time. If we neglect damping and, as a first approximation, consider the equations to be uncoupled for each node, the *DAF* of the displacements can be considered as the maximum of:

$$DAF = \frac{x_d}{x_s} = \frac{F - M\ddot{x}_d}{F} \tag{4}$$

Thus, in this simplified model the *DAF* depends only on the wave forcing F and on the inertia of the structure $M\ddot{x}_d$. We computed this simplified *DAF* for Model 1 at three locations along the water column (z = 43.4, 24.8 and 6.2 m) using the wave kinematics to compute F and the structure acceleration $\ddot{x}_d$ computed by SESAM. The results are given in Table 3 along with those computed by SESAM (Fig. 8). While the analytical values are only of the same order, the increasing trend up the water column is maintained, despite the simplifications in Eq.(4). Therefore, we can conclude that the inertia of the structure has a relevant role on the increase of the *DAF* up the water column.

Vertical position	Simplified DAF	DAF from SESAM
z = 43.4 m	3.49	2.80
z = 24.8 m	3.21	2.75
z = 6.2 m	1.90	2.70

Table 3 *DAF* for displacements in three vertical positions in the water column (Model 1)

As a further verification of this statement we modified Model 1 by changing its mass at the top. In particular, we analyzed two new configurations with SESAM. The first is Model 1 with no mass at the top (Model 1*a*). The second is Model 1 with the same mass as Model 2 (Model 1*b*). We maintained the same natural period of T_n =2.5 s for both Models 1*a* and 1*b*, by changing the stiffness through adjusting Young's modulus E (see Table 4). By doing so the cross-section of each model remains the same and the structures are still drag-dominated.

Models	Top mass [t]	E [N/m^2]
M_1	6.6	2.10 e+11
M_{1a}	0.0	1.63 e+11
M_{1b}	220.9	1.76 e+12

Table 4 Top masses and Young's modulus for Model 1 and its modifications

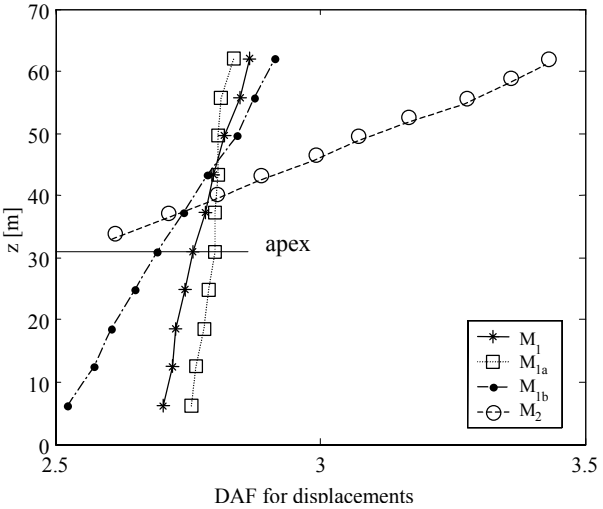

Figure 9 *DAF* for displacements for different top masses and same natural period as a function of the vertical position in the water column

Figure 9 shows the *DAF* for lateral displacements of Models 1, 1*a*, 1*b*, and 2 as a function of the vertical position in the water column. The slope of the *DAF* for Model 1 increases when the top mass becomes larger (Model 1*b*) and becomes almost zero when there is no mass at the top (Model 1*a*). This confirms our

previous conclusions about the importance of the structure's inertia in determining the *DAF*'s slope up the water column. On the other hand, even if Model 2 has the same top mass and the same natural period as Model 1*b*, its *DAF* exhibits a significantly larger slope (Fig. 9). Therefore, the particular structural configuration is in itself responsible for a stronger dynamic sensitivity up the water column, which cannot simply be explained by adopting a model with the same top mass and natural period.

As done for displacements, we analyzed the trend of bending moment along the water column for Models 1, 2 and 3, as the moments are the most important parameter for the design of these structures. Fig. 10 shows the *DAF* for moments as a function of the vertical position in the water column. The *DAF* of Models 2 and 3 reaches very large values (9 and 17, respectively) in the upper part of the wave zone, while from the apex to the still water level the values of the DAF for the three models are more similar. As expected from the previous discussion and from Figs. 6 and 8, Model 3 has a larger *DAF* than Model 2. Whereas displacements at any point are related to the entire structural response, quasi-static bending moments in the caisson are a function of only the loading above the point in question. This difference is one cause of the very large *DAF*s for moments high up the water column.

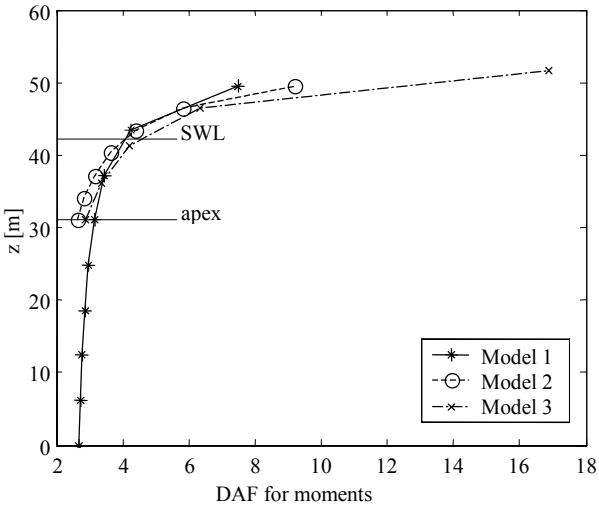

Figure 10 Dynamic amplification factor for moments as a function of the vertical position in the water column

In order to assess the relevance of the results found in this and the previous section, we investigate here the behavior of the *DAF* when the wave period T_w is not an exact multiple of the structure's period T_n. In order to do so, we carried out an analysis of Model 1 for a given wave height (H=20.9 m) and several wave periods, ranging from 9.8 to 18.25 s. Results for displacements at the top and bending moments at the mud-line of the structure are displayed in Fig. 11. Also shown is the *DAF* for the single degree of freedom (SDOF) case, given by the well-known formula:

$$DAF = \frac{1}{\sqrt{\left(1-\left(T_n/T_w\right)^2\right)^2 + \left(2\xi\, T_n/T_w\right)^2}} \qquad (5)$$

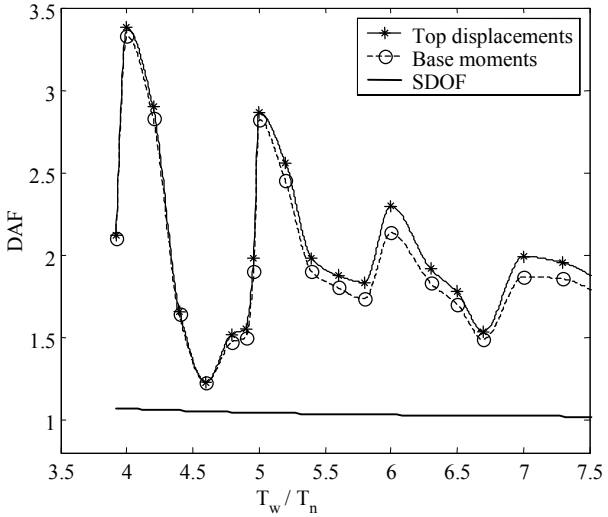

Figure 11 Dynamic amplification factor for top displacements and base moments at different wave periods T_w for Model 1

The effect of the higher wave harmonics can be clearly seen, and the structure is still dynamically excited for T_w/T_n = 7. Moreover, while the *DAF* obviously peaks when T_w is a multiple of T_n, it is also evident that its value is consistently larger than that of the SDOF case also when T_w / T_n is not an integer. While the value of the *DAF* for the SDOF case is close to 1 and almost constant for this range of wave periods, and could therefore discourage a dynamic analysis of the structure, such an analysis is clearly necessary given the behavior of the *DAF* for Model 1.

This shows the importance of the previous results even for the case when T_w is not a multiple of T_n.

CONCLUSIONS

We analyzed the non-linear dynamic behavior of three monopod configurations in a shallow water environment. The wave conditions assumed are typical for Australia's North West Shelf and the Stream function theory of 8th order has been chosen to describe the wave field. The non-linearity is due to three factors: to the wave theory (Stream function), to the drag-force ($u \cdot |u|$ term in Morison's formula) and to the shallow water environment (large H/d). These non-linearities spread the energy of the wave load over higher harmonics.

The dynamic response of each configuration has been compared in terms of the power spectral density of the forcing

function and the dynamic amplification factor (*DAF*). We found that braced monopods (Models 2 and 3) are dynamically more sensitive than the more common analytical model of a vertical cylinder. The power spectral density of the static response has shown that Models 2 and 3 have more energy at higher frequencies than Model 1. They can be dynamically excited by a wave with a period 4 or 5 times their natural period more easily than Model 1. Thus, a dynamic analysis is essential for this kind of structure even if the wave frequency is very different from the first natural frequency and even if the *DAF* for the equivalent single degree of freedom is only marginally larger than unity.

This dynamic sensitivity and non-linear behavior of Models 2 and 3 is also reflected by the increase up the water column of the *DAF* for both displacements and moments. Moreover, we showed that the mass on the top of the structure plays an important role on the increase of the *DAF* up the water column.

The results highlight some key parameters influencing the dynamic response of minimum structures. These conclusions do not by themselves carry direct implications with respect to design. However, they form the fundamental premise for an investigation on the dynamic response of these structures in random seas, which forms the next step of this research.

ACKNOWLEDGMENT

This work was undertaken as part of a research project within the Cooperative Research Centre for Welded Structures (CRC-WS), whose support is gratefully acknowledged. The entire project has been possible thanks to an International Postgraduate Fee Exemption Scholarship and a University of Western Australia Postgraduate Award. Thanks to DNV and to Aanund B. Berdal in particular, for the excellent technical support in using SESAM.

REFERENCES

Baltrop, N.D.P. & Adams, A.J. 1991, *Dynamics of fixed marine structures*, 3rd Ed. Butterworth-Heinemann, Oxford.

Borgman, L.E. 1969, 'Ocean wave simulation for engineering design', *J. Waterways and Harbours Div*., ASCE, WW4, November.

Clough, W.R. & Penzien, J. 1975, *Dynamics of structures*, McGraw-Hill Kogakusha Ltd, Tokyo.

Dean, R.G. 1965, 'Stream function representation of nonlinear ocean waves', *J. of Geophysical Research*, vol. 70, no.18, pp. 4561-4572.

Nedergaard, H., Tychsen, J. & Lyngesen, S. 1996, 'Ringing and double frequency response of a tripod', *OMAE Proceedings*, ASME, vol. 1, part A, pp. 497-505.

Pierson, W.J. & Holmes, P. 1965, 'Irregular wave forces on a pile'*, J. Waterways and Harbours Div.*, ASCE, vol.91, WW4.

Ronalds, B.F., Wong, Y.T., Tuty, S. & Piermattei, E.J. 1998, 'Monopod reliability offshore Australia', *Proc. 17th Int. Conf. OMAE*, ASME, Lisbon.

Ronalds, B.F., Anthony, N.R., Tuty, S. & Fakas, E. 2000, 'Monopod structural reliability under storm overload', *Proc. Joint Conf. ETCE/OMAE, ASME*, New Orleans.

Ronalds, B.F., Tuty, S., Pinna, R., Cole, G.K. & Fakas, E. 2001, 'Platform configuration and structural reliability relationship', *Proc. Int. Conf. on Safety, Risk and Reliability – Trends in Engineering*, IABSE, Malta.

Steedman Science & Engineering, 1994, *Oceanographic and meteorological design criteria – Wandoo location*, Report R590.

Tuty, S., Ronalds, B.F., Harding, J.R. & Fakas, E. 2001a, 'Storm overload response of North West Shelf monopods', *Proc. Int. Conf. on Safety, Risk and Reliability –Trends in Engineering*, IABSE, Malta.

Tuty, S., Cassidy, M.J. & Ronalds, B.F. 2001b, 'Investigation of shallow water kinematics and local effects on reliability of minimum structures'*, Proc. 20th Int. Conf. OMAE*, ASME, Rio de Janeiro.

Williams, M.S., Thompson, R.S.G. & Houlsby, G.T. 1999, 'A parametric study of the non-linear dynamic behavior of an offshore jack-up unit', *Engineering Structures*, vol. 21, pp. 383-394.